APPENDICE B

INTERNATIONAL CONFERENCES

1. **Supasit Paengson,** Chanchana Thanachayanon and Tosawat Seetawan. "Thermoelectric Power Generation of $Ca_{0.97}Bi_{0.03}MnO_3$ N–Type Thermoelectric Module". Siam Physics Congress 2014 (SPC 2014), 26–29 March 2014, Poster presentation.

2. **Supasit Paengson,** Kunchit Singsoog, Panida Pilasuta, Wanatchaporn Namhongsa, and Tosawat Seetawan. "P–$Ca_3Co_4O_9$+Ag and N–$Ca_{0.97}Bi_{0.03}MnO_3$ Materials for Thermoelectric Generation". The 3rd Southeast Asia Conference on Thermoelectrics 2014 (SACT 2014), 22–24 December 2014, Oral presentation.

4. **Supasit Paengson,** Panida Pilasuta, Kunchit Singsoog, Wanatchaporn Namhongsaand Tosawat Seetawan. "Comparative power generation of uni–leg and π–shape thermoelectric module". Sakon Nakhon Rajabhat University International Conference 2015 (SNRU–IC 2015), 24 July 2015, Poster presentation.

3. **Supasit Paengson,** Kunchit Singsoog, Panida Pilasuta, Wanatchaporn Namhongsa, and Tosawat Seetawan "Improvement in thermoelectric properties of $CaMnO_3$ by Bi doping and hot pressing . International Conference on Science and Technology of emerging materials (STEMa2016), 27–29 July 2016, Poster presentation.

APPENDICE C

PUBLICATIONS

First Author

1. **Supasit Paengson**, Panida Pilasuta, Kunchit Singsoog, Wanatchaporn Namhongsa Wairut Impho and Tosawat Seetawan. "Improvement in thermoelectric properties of $CaMnO_3$ by Bi doping and hot pressing" Materials Today Proceedings **(Accepted) (Scopus)**

2. **Supasit Paengson,** Kunchit Singsoog, Panida Pilasuta, Wanatchaporn Namhongsa, and Tosawat Seetawan, P–$Ca_3Co_4O_9$ Doped Ag and N–$Ca_{0.97}Bi_{0.03}MnO_3$ Materials for Thermoelectric Refrigerator. J. Mater. Sci. Appl. Energ. 4(1), 9–12, (2015).

STEMa2016

Improvement in thermoelectric properties of CaMnO₃ by Bi doping and hot pressing

Supasit Paengson[a,b], Panida Pilasuta[a,b], Kunchit Singsoog[a,b], Wanatchaporn Namhongsa[a,b] Wairut Impho [b,c], Tosawat Seetawan[a,b]*

[a]Program of Physics, Faculty of Science and Technology, Sakon Nakhon Rajabhat University, 680 Nittayo Rd., Mueang District, Sakon Nakhon, 47000, Thailand
[b]Thermolectric Research Laboratory, Center of Excellence on Alternative Energy, Research and development institution, Sakon Nakhon Rajabhat University, 680 Nittayo Rd., Mueang District, Sakon Nakhon, 47000, Thailand
[c]Program of Mechanical and industrial Faculty of Industrial Technology, Sakon Nakhon Rajabhat University, Sakon Nakhon, 47000, Thailand

Abstract

The polycrystalline of $Ca_{1-x}Bi_xMnO_3$ (x = 0, 0.01, 0.02, 0.03, 0.04 and 0.05) thermoelectric materials were prepared by solid state reaction (SSR) and hot pressing (HP) methods. The crystallography and morphology were analysed by X-ray diffraction (XRD) and scanning electron microscopy (SEM), respectively. It was found that the lattice parameters of Orthorhombic-perovskite increased with increasing Bi contents. The Seebeck coefficient shows negative value indicated n-type material and decreased with increasing Bi contents. The electrical resistivity decreased with increasing Bi content indicating metallic conduction as well but the thermal conductivity shows the semiconductor behaviour. The dimensionless figure of merit (ZT) value of $Ca_{0.97}Bi_{0.03}MnO_3$ sample shows highest value about 0.065 at 473 K and the ZT value higher than un-doped $CaMnO_3$ sample 95% at same temperature.

Keywords: Oxide thermoelectric material; CaMnO₃; hot pressing; Bi doping, Seebeck coefficient;

* Corresponding author. Tel.: +66 4 274 4319; fax: +66 4 274 4319.
  E-mail address: t_seetawan@snru.ac.th

1. Introduction

The long time of development and intense interest to thermoelectric (TE) materials because TE materials can generate electricity from heat energy directly in the other hand can create hot and cold side by using electricity. The efficiency of thermoelectric material can evaluate by using dimensionless figure of merit (ZT).

$$ZT = \frac{S^2 T}{\rho \kappa} \qquad (1)$$

where S , ρ , κ and T are Seebeck coefficient, electrical resistivity, thermal conductivity and absolute temperature, respectively. For application the thermoelectric, it is necessary to $ZT > 1$, that require large the power factor (PF) and low thermal conductivity.

$$PF = \frac{S^2}{\rho} \qquad (2)$$

Normally, the thermoelectric material in commercial consists of p and n type connect series with metal electrode on ceramic substrates. The commercial TE material mainly use BiTe and PbTe-bases [1,2] for fabrication thermoelectric module which materials an expensive and working in low temperature. Now the trend of development TE material concentrate to wide working temperature range, friendly environment and stability. Oxide thermoelectric material interested from many researcher such as $NaCo_2O_3$, $Ca_3Co_4O_9$, $SrTiO_3$ and $CaMnO_3$ [3-9] etc. However, although in oxide material are large S and κ but also make low ZT because high ρ . Thus in this paper report about decrease ρ from increasing carrier concentration and decreasing oxygen vacancy by increased density from hot pressing method for improvement ZT value [10].

2. Experimental Details

The $Ca_{1-x}Bi_xMnO_3$ (x = 0, 0.01, 0.02, 0.03, 0.04 and 0.05) polycrystalline ceramics were prepared by SSR of calcium carbonate powder ($CaCO_3$ purity 99%) mixed with manganese dioxide (MnO_2 purity 99.9%) and bismuth oxide (Bi_2O_3 purity 99.5%) in stoichiometric ratios. The powders were ball milled in ethanol by zirconia balls for 12 h. The milled powders were calcined at 1273 K for 24 h in air after an intermediate grinding step. Then the powders were hot pressed on graphite die 10 mm diameter pellets and pressure of 60 MPa at a temperature 1173 K 1 h soak time. The pellets were then annealed and remove carbon in air at 1473 K with a 36 h soak time. The crystal structure were characterized by XRD (XRD-6100, Shimadzu) powder equipped with Cu Kα radiation (a step width of 0.020°) angular range 20-80°. The density of the sintered pellets were measured by the Archimedes method. The morphology was obtained by SEM (JSM-7800F, JEOL) and sintered pellets were cut into rectangular columns with dimensions of $3 \times 3 \times 15$ mm^3 for measurement of thermoelectric properties.

The S and ρ were measured by a steady-state technique which calibrate compared with ULVAC-ZEM-3 by constantan standard were performed between 300 and 473 K with a temperature gradient of 0.5 - 1 K across the sample. The temperature different between hot and cold point of sample was use K type thermocouple which was measured using a PICOTEST multimeter. The κ were measured by steady-state technique and calculated by the heat rate ($\dot{Q}$), the surface area of sample (A), the distant between hot and cold probe on sample (x) and temperature different between hot and cold probe (ΔT) following by a relationship.

$$\kappa = -\frac{\dot{Q}}{A} \frac{x}{\Delta T} \qquad (3)$$

The hot and cold points of sample were used K type thermocouple of PICOTEST multimeter and real-time thermal data logger for interface with computer. Then the PF and ZT were calculated.

3. Results and discussion

The X-ray diffraction pattern of sintered $Ca_{1-x}Bi_xMnO_3$ (x = 0, 0.01, 0.02, 0.03, 0.04 and 0.05) ceramics at room temperature, is shown in Fig.1. The diffraction pattern of all ceramics are correspond with $CaMnO_3$ (CMO) un-doped sample phase. All sample no peak of secondary phase were observed corresponding to CMO phase, thus indicating were a single phase with an orthorhombic perovskite structure in *Pnma* space group (PDF Card - 00-050-1746). Lattice parameter were calculated from XRD data meanwhile, the cell volume and theoretical density of all sample tabulated in Table 1. The result of lattice parameter and cell volume increased linearly with increasing Bi doping contents [11]. This behavior was affected from substitution of Bi on Ca-site which similar ionic radius of the element. According to these reported in the $Ca_{1-x}Bi_xMnO_3$ system, Bi sever as electron doping [11,12,16]. Then the electron doping was induced the present by Mn^{3+} within Mn^{4+} matrix of CMO and the difference ionic radius between Mn^{3+} (0.64 Å) was larger than Mn^{4+} (0.53 Å) which distort the octahedral in CMO structure [13-15]. So it was found that lattice the parameter increased with increasing Bi content.

The experimental density in the Table 1 were increased with increasing of doping Bi contents. The density increased because Bi was heavier mass contribution of CMO and another factor used hot pressing method for prepared all sample helpful decreasing porosity on the samples. The theoretical density of all sample was calculated from lattice constant of XRD data and the relative density show good compactness.

The microstructure of bulk $Ca_{1-x}Bi_xMnO_3$ (a) x = 0.00, (b) x = 0.01, (c) x = 0.02, (d) x = 0.03, (e) x = 0.04 and (f) x = 0.05 ceramics, are shown in Fig. 2. The morphology of all sample showed good compactness, and decreased grain connecting of pore and micro-cracking in the sample due to the density increased by using HP method when compare with report [11].
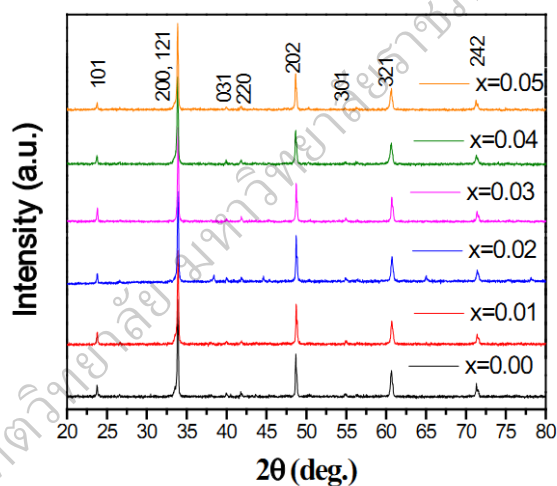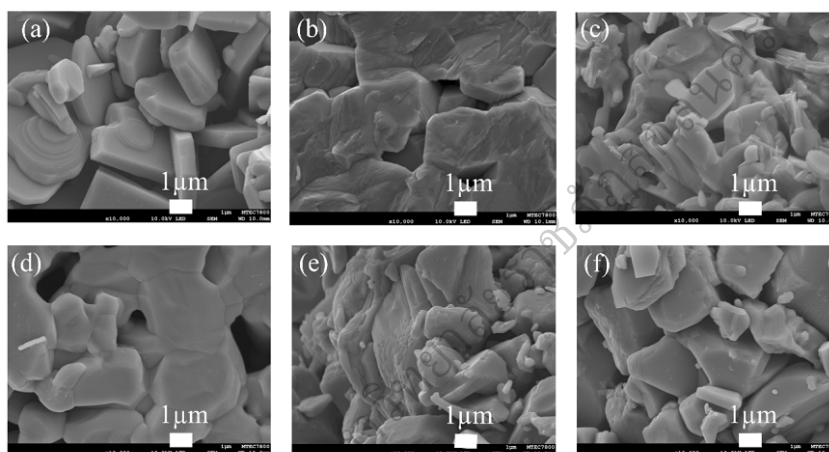

Fig. 1. XRD patterns of $Ca_{1-x}Bi_xMnO_3$ powders for (x = 0.00, 0.01, 0.02, 0.03, 0.04, 0.05) ceramics at room temperature.

114

Table 1. Lattice parameters, densities of $Ca_{1-x}Bi_xMnO_3$ (x = 0, 0.01, 0.02, 0.03, 0.04 and 0.05) ceramics.

Sample Bi content (x)	a (Å)	b(Å)	c(Å)	Unit cell Volume (Å³)	Theoretical density (g/cm³)	Experimental density (g/cm³)	Relative density (%)
0	5.2895	7.4949	5.2257	207.172	4.58	4.25	92.79
0.01	5.2989	7.4679	5.2399	207.338	4.63	4.21	90.92
0.02	5.2801	7.4683	5.2802	208.214	4.67	4.31	92.92
0.03	5.3271	7.4890	5.2466	208.215	4.72	4.34	91.94
0.04	5.2906	7.4685	5.2697	209.312	4.75	4.42	93.05
0.05	5.3161	7.4687	5.2742	209.412	4.80	4.47	93.15

Fig. 2. SEM image of bulk $Ca_{1-x}Bi_xMnO_3$. (a) x = 0.00, (b) x = 0.01, (c) x = 0.02, (d) x = 0.03, (e) x = 0.04 and (f) x = 0.05 ceramics.

The Seebeck coefficient of $Ca_{1-x}Bi_xMnO_3$ (x = 0, 0.01, 0.02, 0.03, 0.04 and 0.05) ceramics were measured by steady state technique at 300 K to 473 K in atmosphere, are shown in Fig. 3 (a). The S of all sample showed negative value, were indicated an n-type electrical conduction behaviour in Fig. 3 (a). The un-doped CMO showed large absolute value of S and typical semiconductor behaviour. On the other hand, all doped samples showed metallic conduction behaviour and the S decreased with increase Bi contents. From this behaviour was attributed the increasing carrier concentration of CMO which observed lattice parameter increased in Table 1, which accord with reported before [11-13]. Thus, the S were evaluated from this equation.

$$S = \frac{\pi^2 k_B^2 T}{e E_F} \qquad (4)$$

where π, k_B, T, e and E_F were Pi, Boltzmann constant, absolute temperature, electron charge and Fermi level, respectively. The S are inversely proportional to Fermi level. From this relation were evaluated by Fermi level from S at 303 K, which were 0.075 eV, 0.184 eV, 0.222 eV, 0.251 eV, 0.275 eV and 0.333 eV for x = 0, 0.01, 0.02,

3. Results and discussion

The X-ray diffraction pattern of sintered $Ca_{1-x}Bi_xMnO_3$ (x = 0, 0.01, 0.02, 0.03, 0.04 and 0.05) ceramics at room temperature, is shown in Fig.1. The diffraction pattern of all ceramics are correspond with $CaMnO_3$ (CMO) un-doped sample phase. All sample no peak of secondary phase were observed corresponding to CMO phase, thus indicating were a single phase with an orthorhombic perovskite structure in *Pnma* space group (PDF Card - 00-050-1746). Lattice parameter were calculated from XRD data meanwhile, the cell volume and theoretical density of all sample tabulated in Table 1. The result of lattice parameter and cell volume increased linearly with increasing Bi doping contents [11]. This behavior was affected from substitution of Bi on Ca-site which similar ionic radius of the element. According to these reported in the $Ca_{1-x}Bi_xMnO_3$ system, Bi sever as electron doping [11,12,16]. Then the electron doping was induced the present by Mn^{3+} within Mn^{4+} matrix of CMO and the difference ionic radius between Mn^{3+} (0.64 Å) was larger than Mn^{4+} (0.53 Å) which distort the octahedral in CMO structure [13-15]. So it was found that lattice the parameter increased with increasing Bi content.

The experimental density in the Table 1 were increased with increasing of doping Bi contents. The density increased because Bi was heavier mass contribution of CMO and another factor used hot pressing method for prepared all sample helpful decreasing porosity on the samples. The theoretical density of all sample was calculated from lattice constant of XRD data and the relative density show good compactness.

The microstructure of bulk $Ca_{1-x}Bi_xMnO_3$ (a) x = 0.00, (b) x = 0.01, (c) x = 0.02, (d) x = 0.03, (e) x = 0.04 and (f) x = 0.05 ceramics, are shown in Fig. 2. The morphology of all sample showed good compactness, and decreased grain connecting of pore and micro-cracking in the sample due to the density increased by using HP method when compare with report [11].
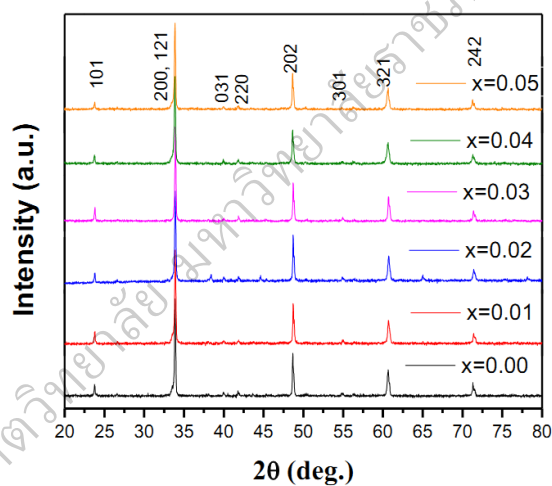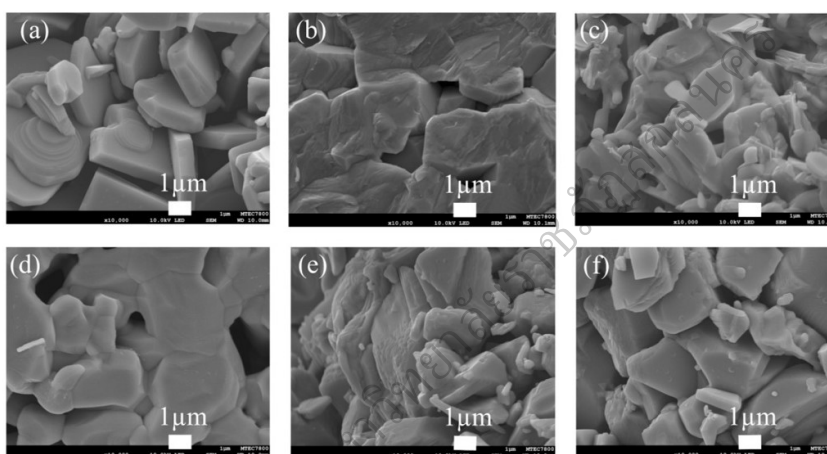

Fig. 1. XRD patterns of $Ca_{1-x}Bi_xMnO_3$ powders for (x = 0.00, 0.01, 0.02, 0.03, 0.04, 0.05) ceramics at room temperature.

Table 1. Lattice parameters, densities of $Ca_{1-x}Bi_xMnO_3$ (x = 0, 0.01, 0.02, 0.03, 0.04 and 0.05) ceramics.

Sample Bi content (x)	a (Å)	b(Å)	c(Å)	Unit cell Volume (Å^3)	Theoretical density (g/cm^3)	Experimental density (g/cm^3)	Relative density (%)
0	5.2895	7.4949	5.2257	207.172	4.58	4.25	92.79
0.01	5.2989	7.4679	5.2399	207.338	4.63	4.21	90.92
0.02	5.2801	7.4683	5.2802	208.214	4.67	4.31	92.92
0.03	5.3271	7.4890	5.2466	208.215	4.72	4.34	91.94
0.04	5.2906	7.4685	5.2697	209.312	4.75	4.42	93.05
0.05	5.3161	7.4687	5.2742	209.412	4.80	4.47	93.15

Fig. 2. SEM image of bulk $Ca_{1-x}Bi_xMnO_3$. (a) x = 0.00, (b) x = 0.01, (c) x = 0.02, (d) x = 0.03, (e) x = 0.04 and (f) x = 0.05 ceramics.

The Seebeck coefficient of $Ca_{1-x}Bi_xMnO_3$ (x = 0, 0.01, 0.02, 0.03, 0.04 and 0.05) ceramics were measured by steady state technique at 300 K to 473 K in atmosphere, are shown in Fig. 3 (a). The S of all sample showed negative value, were indicated an n-type electrical conduction behaviour in Fig. 3 (a).The un-doped CMO showed large absolute value of S and typical semiconductor behaviour. On the other hand, all doped samples showed metallic conduction behaviour and the S decreased with increase Bi contents. From this behaviour was attributed the increasing carrier concentration of CMO which observed lattice parameter increased in Table 1, which accord with reported before [11-13]. Thus, the S were evaluated from this equation.

$$S = \frac{\pi^2 k_B^2 T}{e E_F} \qquad (4)$$

where π, k_B, T, e and E_F were Pi, Boltzmann constant, absolute temperature, electron charge and Fermi level, respectively. The S are inversely proportional to Fermi level. From this relation were evaluated by Fermi level from S at 303 K, which were 0.075 eV, 0.184 eV, 0.222 eV, 0.251 eV, 0.275 eV and 0.333 eV for x = 0, 0.01, 0.02, 0.03,

0.03, 0.04 and 0.05, respectively. This result mean the Bi doping were increased Fermi level of CaMnO$_3$ un-doped. When Ca^{2+} substituted Bi^{3+} which the Bi^{3+} was a donor ions. Then the increasing of carrier concentration has a directly result to shift of occupied energy level structure to higher binding energy. Therefore, this phenomenal Fermi level increasing was attributed to the increase of Bi doping content [10].

The electrical resistivity of Ca$_{1-x}$Bi$_x$MnO$_3$ (x = 0, 0.01, 0.02, 0.03, 0.04 and 0.05) ceramics, seem in Fig. 3 (b). The ρ of un-doped CMO was deceased with increasing temperature indicate of semiconductor behaviour. However, all doped samples showed ρ was increased with increasing temperature indicate metallic behaviour and also the ρ decreased with increasing doped Bi contents. Because the effect from Bi serving increased carrier concentration according with previous work [10,15].

The power factor of all sample were evaluated by S and ρ as equation (2). The un-doped sample showed lowest PF due to high S but in ρ is very high when compared with doped sample. The maximum of PF shows in condition Ca$_{0.99}$Bi$_{0.01}$MnO$_3$ about 5.7×10^{-4} W m^{-1} K^{-2} and the trend of all doped sample increased with increasing temperature.

The total thermal conductivity (closed symbols) and electronic thermal conductivity (open symbols) for all sample at temperature range of300 to 473K, as shown in Fig. 4 (a). The total thermal conductivity (κ) were evaluated by combination lattice thermal conductivity (κ_l) and electronic thermal conductivity (κ_e). The electronic thermal conductivity was calculated from Wiedemann-Franz's law equation by using electrical resistivity.
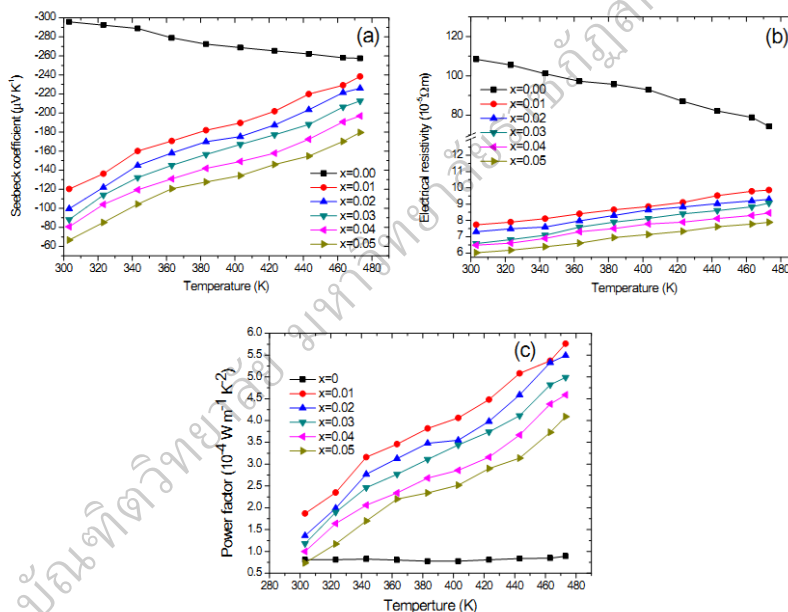

Fig. 3. The relationship between temperature dependent and (a) the Seebeck coefficient; (b) the electrical resistivity and (c) the power factor for Ca$_{1-x}$Bi$_x$MnO$_3$ ceramics.

$$\kappa_e = \frac{LT}{\rho} \qquad (3)$$

where κ_e, L, T and ρ are electronic thermal conductivity, Lorentz constant, absolute temperature and electrical resistivity, respectively. The κ_e of all sample doped were increased with increasing temperature as well as of doped Bi contents [11]. Then compared between κ, it was clearly the major of value got from the κ_l. Therefore, the κ with un-doped CMO was compared with all doped samples show lower than un-doped sample indicating that Bi substitution at Ca-site can be decreased of κ. The κ of x= 0.01, 0.02 and 0.03 samples were decreased by reduction of κ_l. The possible about this behavior was that both the crystal distortion and oxygen vacancy contributed to decrease of κ. The strong crystal distortion was created enhance phonon scattering resulting in the decreased of κ. However, the doped sample x>0.03 was increased slightly due to crystal distortion and increased oxygen vacancy shows in the relative density value and main factor for phonon scattering more Bi substitution which increase κ [10,11].

The dimensionless figure of merit of all samples, are shown in Fig. 4 (b). Normally, all doped samples show higher ZT value more than the un-doped CMO. The $Ca_{0.97}Bi_{0.03}MnO_3$ shows highest ZT value about 0.065 at 473 K together with un-doped sample mean 95% at same temperature. Because in this condition lowest κ was 3.60 W m^{-1} K^{-1} and optimized PF.

4. Conclusions

The Bi doping of $Ca_{1-x}Bi_xMnO_3$ for x = 0, 0.01, 0.02, 0.03, 0.04 and 0.05 ceramics were successfully synthesized by SSR and HP method. The crystal structure of all sample show single phase and orthorhombic perovskite structure. The lattice parameters and cell volume were increased with increasing Bi contents and increased density of all samples. The SEM image shows good compactness and connecting grain. Then ρ of all doped samples were decreased with decreasing Bi contents and showed metallic behavior. The κ has been lowest at x = 0.03 of 3.6 W m^{-1} K^{-1} at 473 K. The highest ZT = 0.065 at 473 K was increased more than un-doped $CaMnO_3$ about 95 %. The thermoelectric properties were improved by Bi doping, increasing carrier concentration, and using HP method could increase density of all samples.
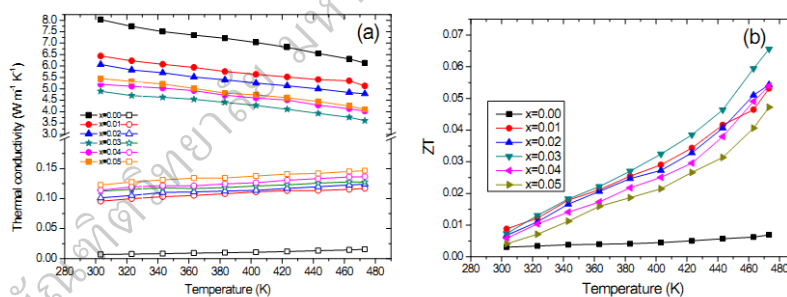

Fig. 4. The relationship between temperature dependent and (a) the total thermal conductivity (closed symbols) and electronic thermal conductivity (open symbols); (b) ZT for $Ca_{1-x}Bi_xMnO_3$ ceramics.

Acknowledgements

References

[1] G. E. Smith, R. Wolfe, J. Appl. Phys. 33 (1962) 841–846.
[2] L. Hua-jun, W. Yun-long, H. Rong-jin, S. Chun-mei, L. Lai-feng, J. Phys. Chem. Solids. 67 (2006) 1492–149.
[3] I. Terasaki, Y. Sasago, K. Uchinokura, Phys. Rev. B. 55 (1997) 12685–12687.
[4] G. J. Xu, R. Funahashi, M. Shikano, I. Matsubara, Y. Q. Zhou, Appl. Phys. Lett. 80 (2002) 3760–3762.
[5] G. Constantinescu, Sh. Rasekh, M. A. Torres, J. C. Diez, M. A. Madre, A. Sotelo, J. Alloy. Compd. 550 (2013) 511-515.
[6] Y. Wang, Y. Sui, J. Cheng, X. Wang, J. Miao, Z. Liu, Z. Qian, W. Su, J. Alloy. Compd. 448 (2008) 1–5.
[7] S. Katsuyama, Y. Takiguchi, M. Ito, J. Mater. Sci. 43 (2008) 3553–3559.
[8] P. P. Shang, B. P. Zhang, J. F. Li, N. Ma, Solid. State. Sci. 12 (2010) 1341–1346.
[9] H. Muta, K. Kurosaki, S. Yamanaka. J. Alloy. Compd. 350 (2003) 292–295.
[10] Y. H. Zhu, W. B. Su, J. Liu, Y. C. Zhou, J. Li, X. Zhang, Y. Du, C. L. Wang, Ceram. Int. 41 (2015) 1535–1539.
[11] R. Kabir, R. Tian, T. Zhang, R. Donelson, T. T. Tan, S. Li, J. Alloy. Compd. 628 (2015) 347–351.
[12] Y. Zhu, C. Wang, H. Wang, W. Su, J. Liu, J. Li, Mat. Chem. Phys. (2014) 385-389.
[13] X. Y. Huang, Y. Miyazaki, T. Kajitani, Solid. State. Comm. 145 (2008) 132–136.
[14] Y. Q. Zhou, I. Matsubara, R. Funahashi, G. J. Xu, M. Shikano, Mater. Res. Bull. 38 (2003) 341.
[15] A. Bhaskar, C. J. Liu, J. J. Yuan, C. L. Chang, J. Alloy. Compd. 552 (2013) 236-239.

Co-Author

1. Kunchit Singsoog, Panida Pilasuta, **Supasit Paengson**, Wanachaporn Namhongsa, Weerasak Charoenrat, Surasak Ruamruk, Wiruj Impho, Phanuwat Wongsangnoi, Wasana Kasemsin and Tosawat Seetawan. "THE EFFECT OF SILVER AND BISMUTH DOPED Mg2Si ON CRYSTAL TRUCTURE AND THERMOELECTRIC PROPERTIES". Journal of Materials Science and Applied Energy. 6(1), 102–105, (2017) **(TCI 2)**

2. Panida Pilasuta, Kunchit Singsoog, Supasit Paengson, Wanatchaporn Namhongsa, Phanuwat Wongsangnoi, Wairut Impho, Suwipong Hemathulin, Sakorn Inthachai and Tosawat Seetawan. "Effect of dopant on thermal conductivity of ZnO. Suranaree". J. Sci. Technol. 23(1), (2016) 11–15. **(AGRIS, ACI)**

3. Panida Pilasuta, Kunchit Singsoog, **Supasit Paengson**, Wanatchaporn Namhongsa, Ladapa Sripasuda, and Tosawat Seetawan. "Enhancement of thermoelectric properties induced by Co in ZnO". Suranaree J. Sci. Technol. 23(1), (2016), 25–29. **(AGRIS, ACI)**

4. Kunchit Singsoog, Panida Pilasuta, **Supasit Paengson**, Wanatchaporn Namhongsa, Chanchana Thanachayanont, Anek Charoenphakdee, Weerasak Charoenrat and Tosawat Seetawan. "Enhancement of thermoelectric properties of $Sr_{1-X}La_XTiO_3$ (X=0, 0.08, 0.13). Suranaree J. Sci. Technol. 23(1), (2016), 31–35. **(AGRIS, ACI)**

5. W. Namhongsa, K. Singsoog, **S. Paengson**, P. Pilasuta, T. Seetawan, P. Muthitamongkol, and C. Thanachayanont. "Thermoelectric Materials Effects of Magnetic Field on Synthesis and Thermoelectric Properties of $NaCoO_2$". Integrated Ferroelectrics: An International Journal, 165(1), 81–85, (2015). **(ISI Web of Knowledge, Impact factor (2015) = 0.375)**